Performance Analysis of Kalman Filter as an Equalizer in a non-Gaussian environment

Ly Thi Khanh Vu
School of Electrical Engineering
Vietnam International University
Ho Chi Minh City, Vietnam
vuthikhanhly8396@gmail.com

Huu Tue Huynh
Department of Electrical and Computer Engineering
Laval University
Ste-foy, Quebec, G1K 7P4 Canada

Hung Ngoc Do
School of Electrical Engineering
Vietnam International University
Ho Chi Minh City, Vietnam

2022 IEEE Integrated STEM Education Conference (ISEC) | 978-1-6654-8429-9/22/$31.00 ©2022 IEEE | DOI: 10.1109/ISEC54952.2022.10025219

Abstract*—This paper analyzed the MSE and BER performances of communication systems which used Kalman Filtering as a channel equalizer in non-Gaussian noise environment. In telecommunication systems, fading and additive noise are two critical factors that significantly impacts on the system performance. Most of existing receiver have been designed to well-handle the AWGN noise, thus, such systems may suffer several performance losses when other noise types as impulsive noises present. The proposed algorithm applies the Kalman filter-based equalizer to overcome the impact of non-Gaussian noise. Multiple non-Gaussian noise models have been developed, among them, Middleton's Class A noise is chosen in the scope of this paper. A Rayleigh flat-fading channel is simulated using autoregressive model approach which makes Kalman filtering being usable. The BER and MSE performances of Kalman equalizer under subjected non-Gaussian noise is analyzed for various SNR and parameters scenarios. Simulation results show that the performance of Kalman equalizer is impacted by the overlapped index and the ratio of Gaussian noise power over Impulsive noise power under class A noise. In the high SNR region, BER performance is significantly impacted by impulsive component and in the low SNR region, the performance is mainly impacted by Gaussian component.

Keywords*—Kalman Filtering, Impulsive noise, Middleton's Class A, Autoregressive model, Rayleigh flat-fading.

I. Introduction

In telecommunication, fading and additive noise are two critical factors that significantly impact on the system performance. Fading degrades the transmitted signal power due to various obstacles in transmission. In additional, the radio environment is results of man-made noise sources such as television, network interference, mobile [1], etc. Which leads to the induce of non-Gaussian environment. Most of designed receivers can well-handle the AWGN noise, however, performance of such systems may deteriorate with the injection of other noise types such as impulsive noise. Impulsive noise is seriously harmful to the system performance due to the impulses causing the burst of errors into the information bits. However, their impacts are sometimes overlooked. Many algorithms have been proposed to resolve the problem of impulse noise, among them, an algorithm uses Kalman filter as a channel equalizer at the receiver is proposed. Even Kalman filter is only optimal in case of LTI system with the presence of Gaussian noise, it can still be used as an estimator in other cases. The application of Kalman filter recursive algorithm aims to estimate channel coefficients based on the time evolution of the communication system, given noisy measurements with the presence of Middleton Class A noise type.

Resolving the Kalman Filter-based equalizer has several challenges since non-Gauss is a tough field both in model and in computation such that rarely publications have been found. Even the most famous research works in the 1970s only considered the MSE performance [8]. However, the presence of MSE only does not mean much in terms of telecommunication. Until 2010, SER performance of communication system is mentioned in several research work, however, these are not common due to lack of methodology. In this paper, an AR modelling approach for representing the Rayleigh channel is implemented [4]. The modulated signal passed through Rayleigh flat-fading channel becoming the input of the Kalman equalizer, which has structure consisting of Kalman filter and MMSE filtering. While the Kalman filter was applied to estimate the channel gains, the MMSE filter reverses the channel effects by minimizing the mean square error criteria. Performance of Kalman channel equalizer in terms of MSE and BER/SER are analyzed and evaluated based on variation of SNR and parameters.

II. Channel model and non-gaussian noise model

A. Channel Model

The Rayleigh channel in wireless communication can be modeled by many approaches such as Sum of Sinusoids (SoS), Inverse Discrete Fourier Transform (IDFT), or Autoregressive (AR) modelling approach. AR modelling approach is chosen because of various reasons. First, AR has a correlation matching property with simple structure. Second, AR requires less storage than IDFT approach. In additional, the use of Kalman computer algorithm requires the presence of time evolution model of state. The AR mathematical model is described as follows [3], [4]:

$$x[n] = -\sum_{k=1}^{p} a_k x[n-k] + w[n] \tag{1}$$

Where the $w[n]$ is the complex white Gaussian noise. The AR model parameters consist of AR parameter$\{a_k\}$ ($k = 1,2 \dots p$) and the variance σ_p^2.

A high accuracy model to describe Rayleigh statistical property has been developed by Jake and Clark, which yields the received fading signals has ACF and the corresponding PSD as follows [13], [14]:

ACF:

$$R[k] = J_0(2\pi f_m \tau) \tag{2}$$

PSD:

$$S(f) = \begin{cases} \dfrac{1}{\pi f_d \sqrt{1-\left(\frac{f}{f_d}\right)^2}}, & |f| \le f_d \\ 0, & |f| > f_d \end{cases} \tag{3}$$

Where $f_m = f_d T$ is the normalized maximum Doppler frequency, f_d is the maximum doppler frequency, and J_0 is the zeroth-order Bessel function of the first kind

The AR parameters can be obtained by applying Yule-Walking equations

$$\boldsymbol{R}_{xx}\boldsymbol{a} = -\boldsymbol{v} \text{ or } \boldsymbol{a} = \boldsymbol{R}_{xx}^{-1}\boldsymbol{v} \tag{4a}$$

$$\boldsymbol{R}_{xx} = \begin{bmatrix} R_{xx}[0] & R_{xx}[-1] & \cdots & R_{xx}[-p+1] \\ R_{xx}[1] & R_{xx}[0] & \cdots & R_{xx}[-p+2] \\ \vdots & \vdots & \vdots \ddots & \vdots \\ R_{xx}[p-1] & R_{xx}[p-2] & \cdots & R_{xx}[0] \end{bmatrix}$$

$$\boldsymbol{a} = \left[a_1\ a_2 \ldots\ a_p\right]^T$$

$$\boldsymbol{v} = \left[R_{xx}[1]\ R_{xx}[2]\ \ldots\ R_{xx}[p]\right]^T \tag{4b}$$

Once having unique solution of $\boldsymbol{a}$, the variance σ_p^2 can be defined as:

$$\sigma_p^2 = R_{xx}[0] + \sum_{m=1}^{p} a_k R_{xx}[-k] \tag{5}$$

The approximated AR autocorrelation matrix is as below:

$$\hat{R}_{xx}[m] = \begin{cases} R_{xx}[0] + \epsilon, m = 0 \\ R_{xx}[m],\ m = 1,2 \ldots p \end{cases} \tag{6}$$

Note that the R_{xx} is of the Toeplitz type of the ACF by JC model.

B. Middleton Class A Noise Model

Among the impulsive noise models, Middleton Class A noise is widely used in the literature [2], [6], [7]. The pdf of the Middleton Class A noise is given as:

$$f_x(x) = \sum_{m=0}^{\infty} P_m N(x; \mu, \sigma_m^2) \tag{7}$$

$N(x; \mu, \sigma_m^2)$ expresses Gaussian pdf with mean μ and variance σ_m^2 in which the sample x_k is taken. The γ is denoted the overlapped index which is the average number of m impulses obtained in the detection intervals, this parameter is occurring according to the Poisson distribution. The expression of $N(x_k; \mu, \sigma_m^2)$ and P_m are given as in the equations (8) and (9).

$$N(x; \mu, \sigma_m^2) = \frac{1}{\sqrt{2\pi\sigma_m^2}} e^{-\frac{x^2}{2\sigma_m^2}} \tag{8}$$

$$P_m = \frac{\gamma^m e^{-\gamma}}{m!} \tag{9}$$

The variance σ_m^2 is defined by the equation (10)

$$\sigma_m^2 = \frac{\sigma_I^2 m}{\gamma} + \sigma_g^2 = \sigma_g^2\left(\frac{m}{\gamma\beta} + 1\right) \tag{10}$$

The σ_I^2 and σ_g^2 are corresponding to the power of impulsive component and the power of Gaussian component. The β is the ratio of Gaussian noise power to non-Gaussian noise power, which is defined by the equation (11):

$$\beta = \sigma_g^2 / \sigma_I^2 \tag{11}$$

Obviously, the statistic property of Class A noise is mainly dependent on the ratio β and the impulsive index γ. If the β is large, the unwanted signal approaches Gaussian process, otherwise, it tends to Poisson process. Similarly, the increase of impulsive index γ leads the noise approaches Gaussian and vice versal. The figures 2.1 and 2.2 show the distribution of noise samples when the two parameters variate.

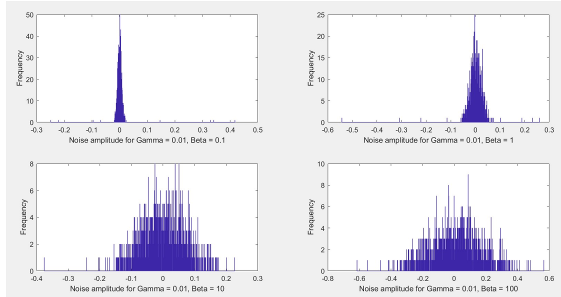

Figure 2.1: Histogram of Middleton Class A noise model for fixed impulsive index $\gamma = 0.01$ and β variates

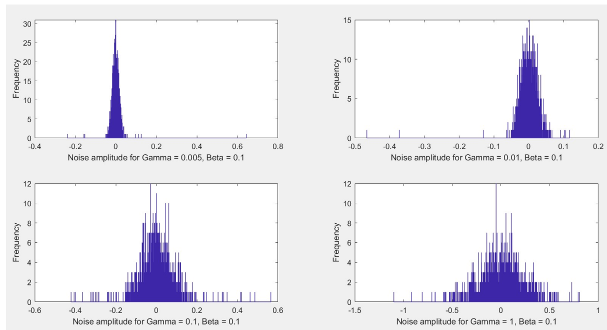

Figure 2.2: Histogram of Middleton Class A noise model for fixed β = 0.01 and γ variates

The presence of impulsive noise on the communication systems which are mainly designed to overcome the AWGN noise will lead to performance loss [15]. It can be shown in the figure 2.3 where the BER performance of BPSK results bad response causing by the presence of impulsive component.

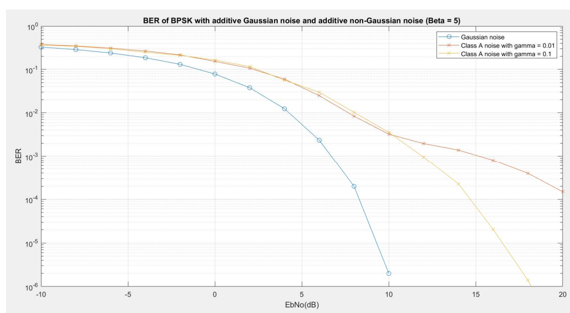

Figure 2.3: BER of BPSK under AWGN and Additive Class A noise ($\beta = 5$)

III. KALMAN FILTERING-BASED CHANNEL EQUALIZER

A. Block Diagram of Baseband Communication System

In this paper, a baseband communication system is proposed where the data is transferred through the Rayleigh flat-fading channel which is simulated by AR modelling approach. The observations include transmitted signal plus non-Gaussian noise. At the receiver, a channel equalizer is applied for time varying channel. While the Kalman filter is used to estimate the channel tap-gains and then the MMSE filter is applied to recover the original signal from the estimated Kalman signal. The figure 3.1 shows the block diagram of proposed system.

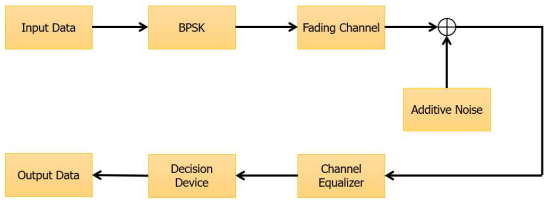

Figure 3.1: Block diagram of baseband communication system

B. *Kalman Channel Equalizer*

The Kalman filter is a computer recursively algorithm which used for state estimation [5], [11]. The idea of using Kalman filter to track the channel coefficients have been investigated in [10], [12], [16] and many other publications, however, most considered using KF under Gaussian environment. The proposal KF equalizer in this paper applied in non-Gaussian environment.

At receiver, the noisy observation is defined as:

$$y(n) = h(n) * x(n) + v(n) \qquad (12)$$

The $h(n)$ represents the channel gains, and $v(n)$ represents the additive non-Gaussian noise. The measured signal $y(n)$ becomes input of the channel equalizer. The channel equalizer then performs two main tasks: estimation of channel gains and recovering of the original signal.

The structure of proposed equalizer includes Kalman filter and a MMSE filter. Which is shown in the figure 3.2.

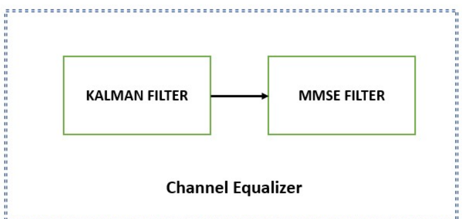

Figure 3.2: Structure of Kalman channel equalizer

- **Kalman Filter**

State-space representations of the proposed system

$$\boldsymbol{x_{k+1}} = \emptyset_k \boldsymbol{x_k} + \boldsymbol{w_k} \qquad (13)$$

$$\boldsymbol{z_k} = \boldsymbol{H_k x_k} + \boldsymbol{v_k} \qquad (14)$$

Given that:

$\boldsymbol{x_k}$: n-state vector at time t_k
$\emptyset_k$: n x n state transition matrix
$\boldsymbol{z_k}$: m-vector observation at time t_k
$\boldsymbol{H_k}$: m x n matrix giving the relationship between state and observation with noise-free at time t_k.
$\boldsymbol{v_k}$: n x 1 vector describing process Gaussian noise with mean 0 and variance Q
$\boldsymbol{w_k}$: m x 1 vector describing measurement non-Gaussian noise with mean 0 and variance R

The covariance matrices for the two Gaussian noises are:
Let $\widehat{\boldsymbol{x}}_{\boldsymbol{k}}^{-}$ be a priori estimate of the state x_k which is defined by

$$\widehat{\boldsymbol{x}}_{\boldsymbol{k}}^{-} = \emptyset_k \boldsymbol{x_{k-1}} \qquad (15)$$

Let $\boldsymbol{P_k^-}$ be the corresponding error covariance matrix of the priori estimate

$$\boldsymbol{P_k^-} = \emptyset_k \boldsymbol{P_{k-1}} \emptyset_k^T + \boldsymbol{Q_k} \qquad (16)$$

The estimation error and the corresponding error covariance matrices can be defined by

$$\boldsymbol{e_k^-} = \boldsymbol{x_k} - \widehat{\boldsymbol{x}}_{\boldsymbol{k}}^{-} \qquad (17)$$

$$\boldsymbol{P_k^-} = E\left[\boldsymbol{e_k^-} \boldsymbol{e_k^-}^{\boldsymbol{T}}\right] = E[(\boldsymbol{x_k} - \widehat{\boldsymbol{x}}_{\boldsymbol{k}}^{-})(\boldsymbol{x_k} - \widehat{\boldsymbol{x}}_{\boldsymbol{k}}^{-})^T] \qquad (18)$$

The posteriori of the desired signal is:

$$\widehat{\boldsymbol{x}}_{\boldsymbol{k}} = \widehat{\boldsymbol{x}}_{\boldsymbol{k}}^{-} + \boldsymbol{K_k}(\boldsymbol{z_k} - \boldsymbol{H_k} \widehat{\boldsymbol{x}}_{\boldsymbol{k}}^{-}) \qquad (19)$$

Note that $(\boldsymbol{z_k} - \boldsymbol{H_k} \widehat{\boldsymbol{x}}_{\boldsymbol{k}}^{-})$ is the difference between the measurement and the priori estimation, also known as the innovation equation. $\boldsymbol{K_k}$ is the Kalman gain at time t_k, also known as a blending factor.
The estimation error and the corresponding error covariance matrix with the posteriori will be

$$\boldsymbol{e_k} = \boldsymbol{x_k} - \widehat{\boldsymbol{x}}_{\boldsymbol{k}} \qquad (20)$$

$$\boldsymbol{P_k} = E[\boldsymbol{e_k} \boldsymbol{e_k}^{\boldsymbol{T}}] = E[(\boldsymbol{x_k} - \widehat{\boldsymbol{x}}_{\boldsymbol{k}})(\boldsymbol{x_k} - \widehat{\boldsymbol{x}}_{\boldsymbol{k}})^T] \qquad (21)$$

The equation for $\boldsymbol{P_k}$ with any gain K is defined as:

$$\boldsymbol{P_k} = (\boldsymbol{I} - \boldsymbol{K_k H_k})\boldsymbol{P_k^-}(\boldsymbol{I} - \boldsymbol{K_k H_k})^{\boldsymbol{T}} + \boldsymbol{K_k R_k K_k}^{\boldsymbol{T}} \qquad (21)$$

The optimal Kalman gain and the respectively optimal error covariance matrix will be

$$\boldsymbol{K_k} = \boldsymbol{P_k^- H_k}\left(\boldsymbol{H_k P_k^- H_k}^{\boldsymbol{T}} + \boldsymbol{R_k}\right)^{-1} \qquad (22)$$

$$\boldsymbol{P_k} = (\boldsymbol{I} - \boldsymbol{K_k H_k})\boldsymbol{P_k^-} \qquad (23)$$

For the next iteration, the estimated state and error covariance matrix are projected ahead to become the initial conditions for the next iteration and the process will go on until the estimation is nearest the true values with acceptable error. The flowchart of Kalman filter is shown in the figure 3.3

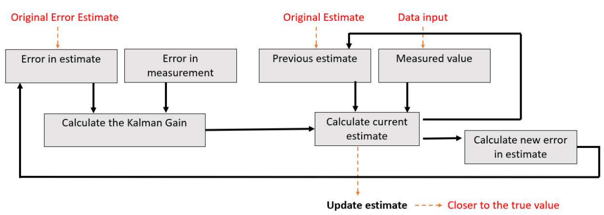

Figure 3.3: Flow chart of Kalman filtering

From equation (13) – (23), the procedure of Kalman filter can be categorized into two main steps: Prediction (Time update) and Correction (Measurement update), which is shown in the figure 3.4.

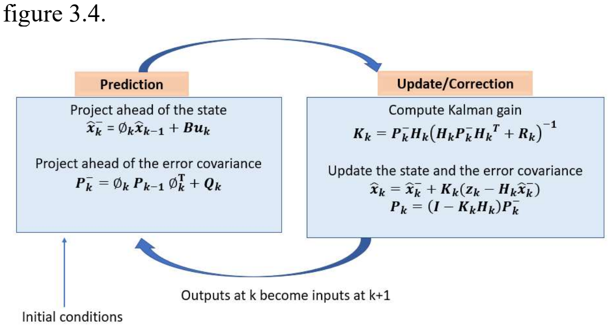

Figure 3.4: Procedure of Kalman filter

- **MMSE Filter**

Once the estimated channel coefficients $\widehat{h_c}$ are ready, the MMSE filter is applied to recover the original transmitted signal by minimizing the mean square error criteria [8] [9]. The designed FIR filter with length N is defined as

$$f(z) = \sum_{k=0}^{N-1} f[k] z^{-k} \qquad (24)$$

The error signal is defined as in equation (25)

$$e[k] = \sum_{i=0}^{N-1} f[i]r[k-i] - u[k-k_0] \quad (25)$$

$$r(n) = \widehat{h_c}(n) * x(n) + v(n) \quad (26)$$

The filter coefficients $\boldsymbol{f}$ can be computed as:

$$\boldsymbol{f} = \left(\boldsymbol{H}^H\boldsymbol{H} + \frac{\sigma_n^2}{\sigma_u^2}\boldsymbol{I}\right)^{-1}\boldsymbol{H}^{\boldsymbol{H}}\delta_{k_0} \quad (27)$$

Note that $\boldsymbol{H}$ is channel matrix ($\boldsymbol{Hf} = \boldsymbol{\delta}_{k_0}$), $\boldsymbol{I}$ is the identity matrix and $\boldsymbol{H}^H$ is Hermitian transpose

The ratio $\frac{\sigma_n^2}{\sigma_u^2}$ inverse of SNR, where σ_n^2 is noise power and σ_u^2 is signal power

δ_{k_0}: column vector $\delta_{k_0} = 1\ at\ k = k_0$, otherwise, $\delta_{k_0} = 0$

Assume that the matrix $\left(\boldsymbol{H}^{\boldsymbol{H}}\boldsymbol{H} + \frac{\sigma_n^2}{\sigma_a^2}\boldsymbol{I}\right)$ is invertible and the receiver has knowledge of $\boldsymbol{H}$, and $\frac{\sigma_n^2}{\sigma_a^2}$

The MMSE is defined as follows:

$$MMSE = \sigma_a^2\left(1 - \delta_{k_0}^T\boldsymbol{H}\left[\boldsymbol{H}^H\boldsymbol{H} + \frac{\sigma_n^2}{\sigma_u^2}\boldsymbol{I}\right]^{-\mathbf{1}}\boldsymbol{H}^H\delta_{k_0}\right) \quad (28)$$

The optimal delay position k_{opt} where the MSE is minimum is then:

$$k_{opt} = argmax\left[diag\left(\boldsymbol{H}\left[\boldsymbol{H}^H\boldsymbol{H} + \frac{\sigma_n^2}{\sigma_u^2}\boldsymbol{I}\right]^{-\mathbf{1}}\boldsymbol{H}^H\right)\right] \quad (29)$$

IV. Results

The simulation of BER/SER and MSE performance of BPSK system which used Kalman channel equalizer for channel estimation and recover the original noise has been conducted. The AR models has AR parameters a = [-0.7711, -0.4855, -0.1999, 0.0856, 0.3710]. The results show that in high SNR area, the system performance is mainly impacted by impulsive component noise, while in low SNR area, the performance is significantly impacted by Gaussian component noise.

A. MSE performance under non-Gaussian environment with γ variates

A test signal contained binary sequence passed through BPSK system is used to estimate the channel coefficients. The observation includes the transmitted signal and the additive impulsive noise. The simulation results give MSE plot versus SNR for in cases the Gaussian noise powers are lower than, equal to, and higher than impulsive noise power, corresponding to $\beta = 0.01, \beta = 1$ and $\beta = 5$. In case of $\beta = 0.01$, the system was mainly impacted by the additive impulsive noise. The variations of γ shows the big MSE differences. For high γ index, the noise is more impulsive and result larger MSE and vice versal. On the other hand, when the power Gaussian noise component is much higher than that of impulsive noise component, the variations of γ do not show any difference now. It can be explained that the additive noise is becoming Gaussian noise for very large β and MSE hardly changed with various γ cases

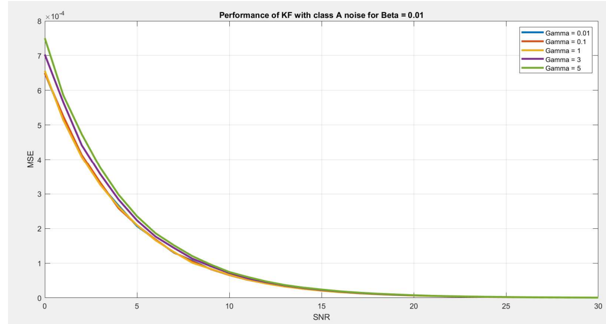

Figure 3.1: MSE versus SNR under non-Gaussian environment with $\beta = 0.01$

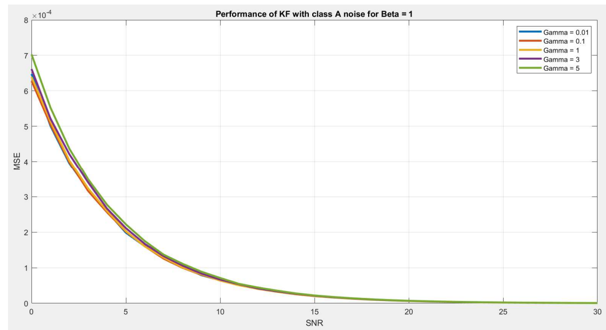

Figure 3.2: MSE versus SNR under non-Gaussian environment with $\beta = 1$

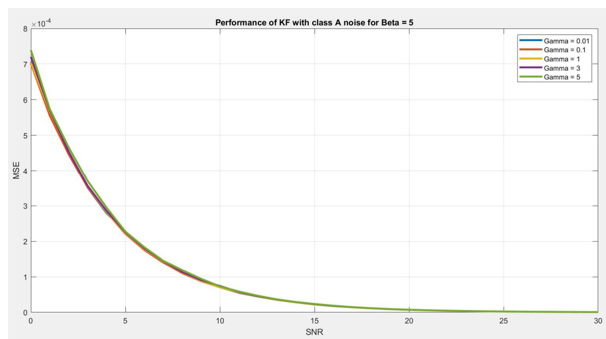

Figure 3.3: MSE versus SNR under non-Gaussian environment with $\beta = 5$

The estimated channel coefficients are tracking closely to the actual channel gains by using KF. The figure 3.4 shows the instantaneous estimation of channel coefficient and its corresponding MSE.

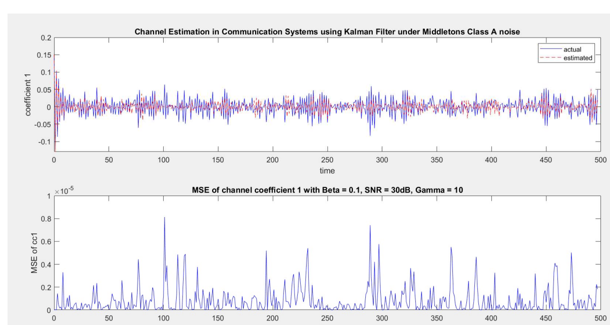

Figure 3.4: Plot of estimated channel coefficient and actual values and the corresponding MSE

B. *MSE performance under non-Gaussian environment with β variates*

The overlapped indexes are corresponding to $\gamma = 0.1$ and 5 in the figures 3.5 and 3.6. Obviously, the variation of β is not affected much on the MSE performance which is comparing to the variation of γ. The lower impulsive index will significantly impact on the MSE performance. For the low impulsive index and low Gaussian to Impulsive noise power ratio, the system is significantly affected by non-Gaussian noise. High values of γ and β lead the system is mainly affected by Gaussian noise.

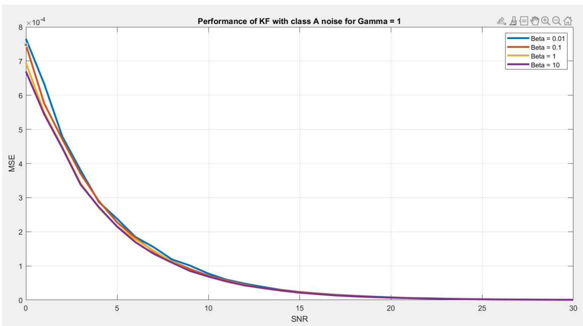

Figure 3.5: MSE versus SNR under non-Gaussian environment with $\gamma = 0.1$

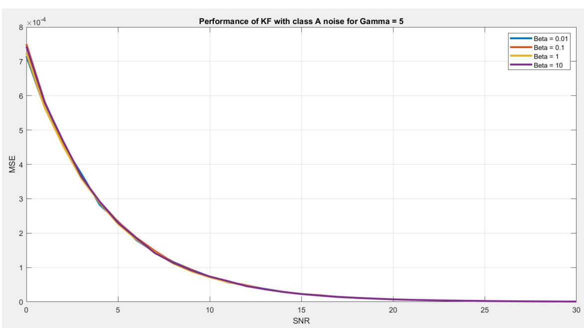

Figure 3.6: MSE versus SNR under non-Gaussian environment with $\gamma = 5$

C. *SER performance under non-Gaussian environment with γ variates*

In the low SNR region, the variations of γ were not impacted much on the SER with the variations of β. In the high SNR region at low β, the low γ values yield high SER since the impulse component significantly impacted on the SER performance of system. At high β, the Gaussian noise power is much higher than the impulsive noise power, the influent regions of Gaussian component and impulsive component were not clear. It can be explained as the β gets bigger, the additive noise is now becoming Gaussian noise according to the central limit theorem. Hence, the SER hardly changes with different values of γ. The simulation results are shown in the figures 3.7 and 3.8

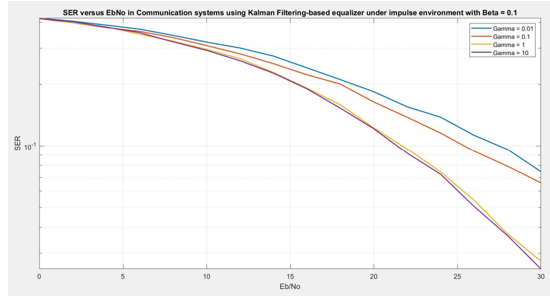

Figure 3.7. SER versus SNR at fixed $\beta = 0.1$ and γ variates

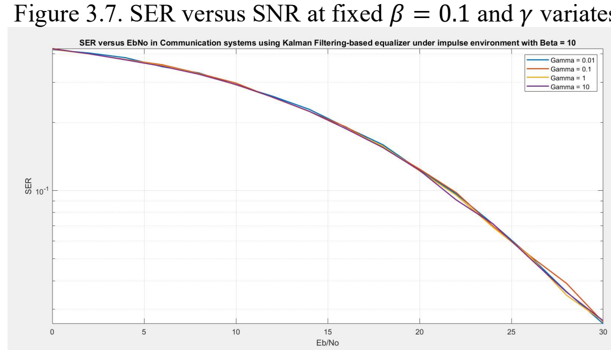

Figure 3.8. SER versus SNR at fixed $\beta = 10$ and γ variates

D. *SER performance under non-Gaussian environment with β variates*

In the low SNR region, the variations of β were not impacted much on the SER. In the high SNR region at low γ, impulsive component significantly impacted on the SER performance of system. With low β values, SER is higher than that of other β values due to the mainly impact of impulsive component, with high β values, the SER is lower than that of other β values due to the significantly impact of Gaussian component.

In case of high overlapped, the influent regions of Gaussian component and impulsive component were not clear. It can be explained as the γ gets bigger, the additive noise is now becoming Gaussian according to the central limit theorem. Hence, the SER hardly changes with different values of β. The simulation results are shown in the figures 3.9 – 3.11

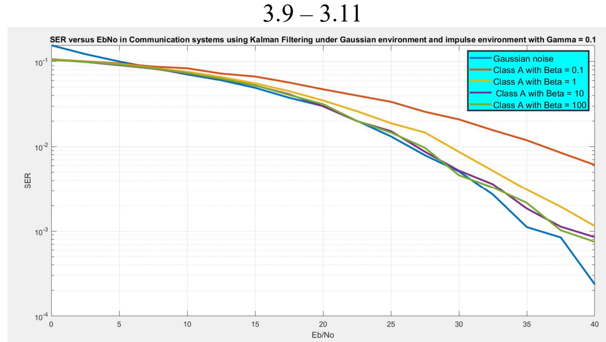

Figure 3.9. SER versus SNR at $\gamma = 0.1$ and β variates

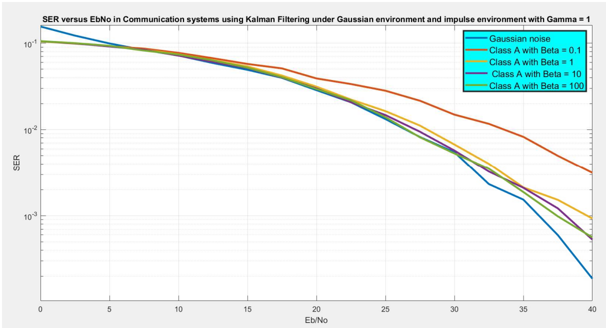

Figure 3.10. SER versus SNR at $\gamma = 1$ and β variates

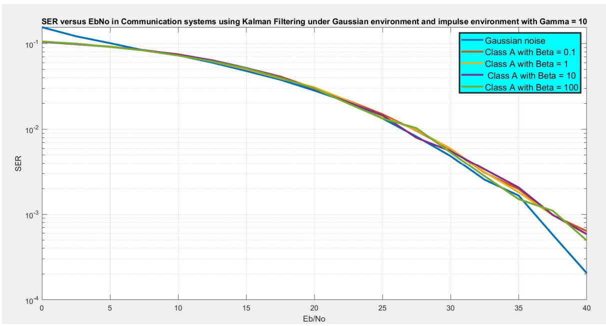

Figure 3.11. SER versus SNR at $\gamma = 10$ and β variates

V. Conclusions

The performance of Kalman filter-based channel equalizer on impulsive environment has been studied. The tracking property of Kalman filter-based equalizer has been performed for the Rayleigh flat-fading channel.

The reliability and accuracy of the communication system is sometimes degraded due to the overlooked of the impact of impulsive noise on the communication system. The SER and MSE performances were affected by the overlapped index (or impulsive index) and the ratio of power of Gaussian over impulsive component.

The proposal of using KF as an equalizer on an impulsive environment yields good MSE and SER performances over the high SNR region. The propose receiver may well-handle both AWGN and additive impulsive noise since it considers either the system is more affected by Gaussian or impulsive noise.

It can be shown that telecommunication system is mainly impacted by Gaussian component over the low SNR region and significantly impacted by Impulsive component over the high SNR region.

References

[1] Frank Leferink, F. Silva, J. Catrysse, S. Batterman, V. Beauvois, A. Roc'h, "Man-made Noise in Our Living Environments," *URSI Radio Science Bulletin*, no. 334, pp. 49-57, Sep 2010.

[2] D. Middleton, "Canonical Non-Gaussian Noise Models: Their Implications for Measurement and for Prediction of Receiver Performance," *IEEE Transactions on Electromagnetic Compatibility,* Vol. EMC-21, no. 3, August 1979.

[3] C.C. Tan and N.C. Beaulieu , "On First-Order Markov Modeling for the Rayleigh Fading Channel," in *IEEE Trans. Commun.*, vol. 48, no. 12, Dec. 2000, pp. 2032-2040.

[4] K.E. Baddour and N.C. Beaulieu, "Autoregressive Modeling for Fading Channel Simulation," in *IEEE Transactions on Wireless Communication*, vol. 4, no. 4, July 2005.

[5] R.E. Kalman, "A New Approach to Linear Filtering and Prediction Problems," in *ASME-Journal of Basic Engineering*, ser. D, 82, pp. 35-45, 1960.

[6] D. Middleton, "Statistical-Physical Models of Electromagnetic Inteference," in *IEEE Transactions on Electromagnetic Compatibility,* vol. EMC-19, no. 3, August 1977.

[7] L. A. Berry,"Understanding Middleton's Canonical Formula for Class A Noise," in *IEEE Transactions on Electromagnetic Compatibility,* vol. EMC-23 no. 4, November 1981.

[8] D. Godard ,"Channel Equalization Using a Kalman Filter for Fast Data Transmission," in *IBM,* pages 267-273, May 1974.

[9] Y. Gong, X. Hong, K.F. Abu-Salim,"Adaptive MMSE Equalizer with Optimum Tap-length and Decision Delay," in *Sensor Signal Process for Defence (SSPD 2010)*, 29-30 Sept. 2010.

[10] R.E Kalman, "A New Approach to Linear Filtering and Prediction Problem," in *Journal of Fluids Engineering*, vol. 82, no. 1, pp. 35-45, 1960.

[11] Q. Li, R. Li, K. Ji and W. Dai "Kalman Filter and Its Applications," ***Intelligent Networks and Intelligent Systems (ICINIS)***, 1-3 Nov. 2015.

[12] X. Zhou, Y. Zhao and X. Zhuang, "Kalman Filter Channel Tracking Algorithm Based on AR Model in WCDMA Systems" in ***WCC 2000 - ICSP 2000. 2000 5th International Conference on Signal Processing Proceedings. 16th World Computer Congress 2000***, 21-25 Aug. 2000.

[13] A. D. Abu Al-Khair and M. M. Banat, "Autoregressive stochastic modeling and tracking of double selective fading channels" in *IASTED International Conference on Communication Systems and Networks*, August 28-30, 2006, Palma de Mallorca, Spain.

[14] S. M. Tawalbeh and M. M Banat, "Simulation of Doubly Selective Fading Channels Using Auoregressive Modeling and Optimum Receiver Design" in *2011 IEEE Jordan Conference on Applied Electrical Engineering and Computing Technologies AEECT*, 6-8 Dec. 2011.

[15] H.T Huynh, P. Fortier, and B. Vo, "Performance Analysis of M-QAM in a non-Gaussian environment," in *International Journal of Electronics and Communications 51*, 255-262.

[16] D. Godard "Channel Equalization Using a Kalman Filter for Fast Data Transmission," in *IBM Journal of Research and Development*, vol. 18, issue. 3, page. 267-273, May 1974.

[17] H. Oh, D. Seo, H. Nam "Design of a Test for Detecting the Presence of Impulsive Noise," in *Sensors*, 12 Dec. 2020.

[18] Zhang. ZG, Chan. SC, Tse. KW "A New Algorithm of Tracking Time-Varying Channels in Impulsive Noise Environment Using a Robust Kalman Filter," in *Proceedings Of 2005 International Sysposium On Intelligent Signal Processing and Communication Systems,* vol. 2005 page. 233-235, 2005.